Monte Carlo Simulation of Growth of Porous SiO_x by Vapor Deposition

V. M. Burlakov,* G. A. D. Briggs, and A. P. Sutton
Department of Materials, University of Oxford, Parks Road, OX1 3PH, United Kingdom

Y. Tsukahara
Technical Research Institute, Toppan Printing Co., Ltd., 4-2-3, Takanodai-gun, Saitama, 345-8508 Japan
(Received 26 September 2000)

A random network model containing defects has been developed and applied to the deposition of amorphous SiOx films on a flat substrate. A new Monte Carlo procedure enables dangling bonds to migrate and annihilate. The degree of porosity in the films is found to increase with oxygen content. As the oxygen content increases a larger fraction of pore surfaces is covered with oxygen, and the density of dangling bonds on pore surfaces decreases. Oxygen plays the role of a surfactant, lowering the energies of pore surfaces and enhancing the porosity of amorphous SiO_2 compared to amorphous Si.

DOI: 10.1103/PhysRevLett.86.3052 PACS numbers: 61.43.Bn, 68.35.–p

Thin layers of nonstoichiometric amorphous silica on polymer films are widely used as gas barrier layers [1]. Porosity of the SiO_x strongly affects the gas barrier performance [2]. We have simulated the growth of amorphous Si and SiO_x layers to understand the chemical and physical factors controlling the porosity. Bulk amorphous Si and SiO_2 structures have been modeled using molecular dynamics simulations [3–5], and Monte Carlo (MC) simulations [6–8]. The MC approach uses two principal ideas: (i) the potential energy of the system is determined by the topology of the bonding configuration, (ii) accessing different bond configurations can be achieved by switching pairs of bonds [6]. By introducing dangling bonds into the continuous random network (CRN) model [9], and a new means of generating alternative bond configurations, we have performed the first MC simulations of the growth of nonstoichiometric SiO_x layers from an atomic vapor. We predict greater porosity in SiO_x than Si films. The surfaces of pores in SiO_x are terminated with oxygen, which reduces their surface energies, and enhances the porosity of the material compared to pure Si.

Amorphous silicon and silicon oxide are network structures, with well-defined local coordination numbers, and weak disorder in terms of bond length and bond angle distributions. The existence of a network structure suggests that valence force field models, such as those due to Keating [10], should be applicable. Recently, such models have been applied to amorphous germanium [6] and silicon [7], and an interface between crystalline silicon and silicon oxide [8]. In these models the potential energy is a function of the bond configuration:

$$E^{\mathrm{CRN}} = \frac{1}{2}\sum_i K^r_{\alpha\beta}(a_i^{\alpha\beta} - a_0^{\alpha\beta})^2 + \frac{1}{2}\sum_i K^\theta_{\alpha\beta\gamma}(\cos\theta_{ij}^{\alpha\beta\gamma} - \cos\theta_0^{\alpha\beta\gamma})^2, \quad (1)$$

where $K^r_{\alpha\beta}$ and $K^\theta_{\alpha\beta\gamma}$ are bond stretching and bond bending force constants ($\alpha, \beta, \gamma = \mathrm{Si}, \mathrm{O}$, and no O-O bonding is assumed to take place), $a_i^{\alpha\beta}$ is the bond length of the ith bond, $a_0^{\alpha\beta}$ is the corresponding equilibrium value, $\theta_{ij}^{\alpha\beta\gamma}$ is the ith bond angle, and $\theta_0^{\alpha\beta\gamma}$ is the corresponding equilibrium value. New configurations are generated by switching pairs of bonds: two bonds AB and CD (A, B, C, and D denote atoms, where A and D are nearest neighbors) are broken, and new bonds AC and BD are created. After each bond-switching event the potential energy, given by Eq. (1), is minimized with respect to bond lengths and bond angles. The new configuration may or may not be accepted, following the usual Metropolis algorithm: if $R < \min\{1, \exp[-(E^{\mathrm{CRN}}_{\mathrm{final}} - E^{\mathrm{CRN}}_{\mathrm{initial}})/kT]\}$ the move is accepted, otherwise it is rejected. Here, R is a random number evenly distributed in the interval $[0, 1]$, k is the Boltzmann constant, and T is absolute temperature. In this scheme no account has been taken of the possibility of dangling bonds.

Dangling bonds are inevitable accidents of growth in real processes. To simulate growth we must go beyond the CRN model by taking into account the energy associated with dangling bonds. The method of generating new bond configurations in the system must also be modified. New configurations are now accessed either by breaking bonds, resulting in creation of pairs of dangling bonds, or by the reverse process of annihilating two dangling bonds on neighboring atoms by forming a bond between them. In addition, isolated dangling bonds are allowed to migrate from one atom to a neighboring atom by forming a bond to the first atom and breaking of a bond to the second. We assign energies $E^d_{\mathrm{Si}} = 1$ eV and $E^d_{\mathrm{O}} = 4$ eV to dangling bonds of silicon and oxygen atoms, respectively. These dangling bond energies are estimates based on the cohesive energies for Si and SiO_2 taken from [11]. The energy of the deposited layer E^D becomes

$$E^D = E^{\mathrm{CRN}} + E^d_{\mathrm{Si}}N^d_{\mathrm{Si}} + E^d_{\mathrm{O}}N^d_{\mathrm{O}} + U_{\mathrm{rep}}. \quad (2)$$

N^d_{Si} and N^d_{O} are the numbers of silicon and oxygen dangling bonds, respectively. Although no silicon atom is allowed more than four bonds, and no oxygen atom is allowed

 0031-9007/01/86(14)/3052(4)$15.00

more than two bonds, it is possible that either may have more than four and two neighbors, respectively, within the second nearest neighbor separation. This is especially likely when rings are formed containing fewer than six oxygen atoms. In that case there are significant repulsive interactions between such atoms, which strongly affect the energetics of small rings. The term U_{rep} is a short-range repulsive interaction designed to penalize Si and O atoms with unbonded atoms within the second nearest neighbor separation. The functional form of U_{rep} is to some extent arbitrary, but we have ensured that our form reproduces the energetics of isolated small rings calculated *ab initio* [12]. Other model parameters were chosen to be the same as in [8] (except θ_0^{SiOSi} which is set equal to 140° in order to maximize agreement with experimental data).

To simulate growth of an SiO_x film we deposited silicon and oxygen atoms from a vapor phase onto an area of 2.4×2.4 nm^2 of an ideally flat substrate with a predetermined density of nucleation sites. Periodic boundary conditions were applied parallel to the substrate. Growth was assumed to be nucleated at sites occupied by unsaturated oxygen atoms that remain firmly attached at random points on the substrate. The simulation of the growth process consists of repeating two sequential steps many times. (1) A silicon or oxygen atom arrives at the growth front, maintaining the required average composition of the SiO_x film, and it is delivered to a randomly selected dangling bond in a surface layer whose thickness depends on the average kinetic energy of the deposited atoms. The thickness of the surface layer was taken to be 10 Å in our simulations. (2) The system was relaxed by MC moves each of which consisted of either the migration of a single dangling bond, or the creation or annihilation of a pair of dangling bonds. Each of these MC steps was followed by full relaxation of the interatomic forces. MC moves were accepted or rejected according to the usual Metropolis scheme using Eq. (2) to define the potential energy of the system, and an effective temperature. To take into account the kinetic energy of the atoms arriving from the vapor phase the effective temperature is taken to be $kT = 0.5$ eV if the MC move involves a recently arrived atom and $kT = 0.05$ eV for any other atom.

We simulated a set of SiO_x structures consisting of 3000 atoms with values of $0 < x < 2$ and for various nucleation site densities. Figure 1 shows a comparison between the radial distribution functions for our simulated amorphous Si and $SiO_{x\simeq 2}$ structures with those obtained from experiment for bulk samples, with the simulated radial distribution functions normalized to account for the reduction in density due to the porosity in our structures. The good agreement between the experimental data and our simulated results enables us to deduce that the structures of the material between the pores in our simulations agree with the structures of bulk samples.

To estimate porosity a cubic mesh of side 0.4 Å was superimposed on the computational cell. A sphere of radius

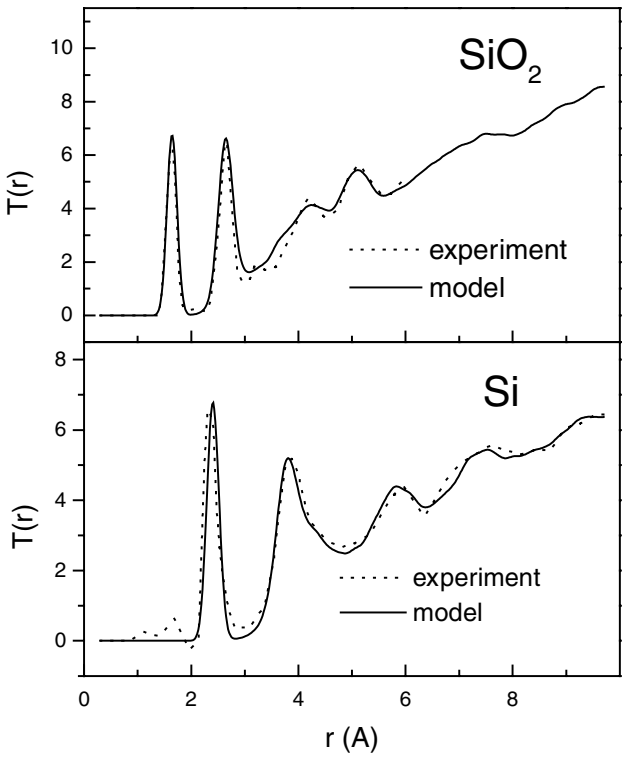

FIG. 1. Radial distribution functions for amorphous SiO_2 and Si. Solid lines are for simulated structures and a convolution was performed with a Gaussian-type instrumental function to obtain the same half-width of the first peak as that of the experimental distribution. Broken lines show experimental data for bulk samples of Si [13] and SiO_2 [4].

2.5 Å was centered on each and every atom in the system. If an elementary cell of the cubic mesh did not overlap with any sphere then the elementary cell was deemed to lie within a pore. The choice of 2.5 Å for the atomic sphere radius ensured that the space within rings containing six oxygen atoms, such as one finds in bulk crystalline SiO_2, is slightly too small to be defined as a pore. We found that porosity varies markedly with the density of nucleation sites. At small nucleation site densities (1.74 nm^{-2}) pores in $SiO_{x\simeq 2}$ can occupy as much as 20% of the film volume, but at larger values (>4 nm^{-2}) porosity reduces to 3%–7% (see Fig. 2). In contrast, porosity in amorphous Si is quite small (<4%) and depends much less on the density of nucleation sites. We have in mind electron beam deposition onto the polymer PET as the substrate, for which the area density of unsaturated oxygens located at carbonyl groups is about 2 nm^{-2} [14]. The pore structures in simulated Si and SiO_2 are shown in Fig. 3, illustrating the strong difference in pore characteristics in these materials.

Why is there so much more porosity in our amorphous SiO_x than in Si? A significant clue is provided by the variation of the composition and dangling bond densities of the surfaces of pores, with the bulk composition of the SiO_x film. In SiO_2 films we find that oxygen atoms account for ≃99% of all atoms on surfaces of pores, and

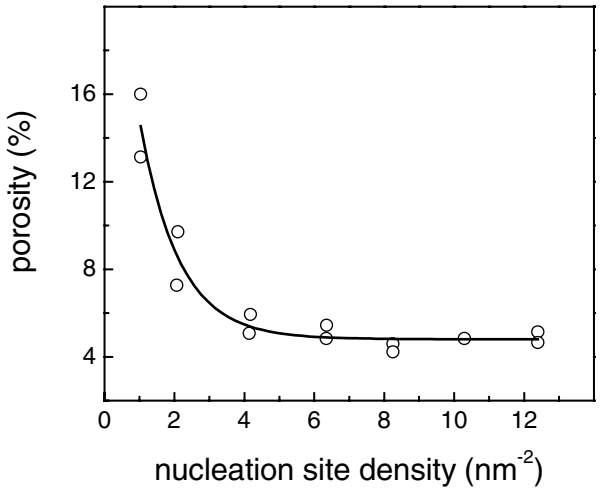

FIG. 2. Calculated porosity in $SiO_{x\simeq 1.8}$ films as a function of assumed nucleation site density on the surface of a model substrate.

dangling bonds appear only on $\simeq$20% of all pore surface atoms. By contrast, in pure Si about 50% of pore surface atoms have dangling bonds. Between these bulk composition limits Fig. 4 shows that the pore surface composition varies monotonically but nonlinearly. Figure 4 also shows that the porosity, averaged over several runs at each composition, increases from $\simeq$2% in pure Si to $\simeq$15% in SiO_2. At the same time we see in Fig. 4 that the fraction of atoms that have dangling bonds on the pore surfaces generally decreases with increasing oxygen content x.

The results in Fig. 4 suggest that oxygen plays a significant role in pore formation kinetics. Oxygen is well suited to the atomic environment of pore surfaces because it is only twofold coordinated. This enables it to form bridges to silicon atoms. In addition, the Si-O-Si bond angle can be deformed at a relatively small energy cost. These factors enable oxygen to saturate dangling bonds of silicon atoms, and thus reduce the energy of pore surfaces. In pure silicon this mechanism is not available for saturating dangling bonds, which therefore remain high in energy. We believe that this is the reason why the porosity of SiO_2 films is greater than that of pure Si.

In previous simulations of porosity only stoichiometric silica was considered, and artificial methods of introducing the porosity were applied to bulk samples, such as scaling the size of the periodic supercell [15], or scaling the effective ionic charges [16]. By contrast, in this work we have simulated growth of thin films and porosity has arisen as a result of realistic processes involving topological defects in the network.

In conclusion, we have carried out simulations of the growth by vapor deposition of amorphous SiO_x films for

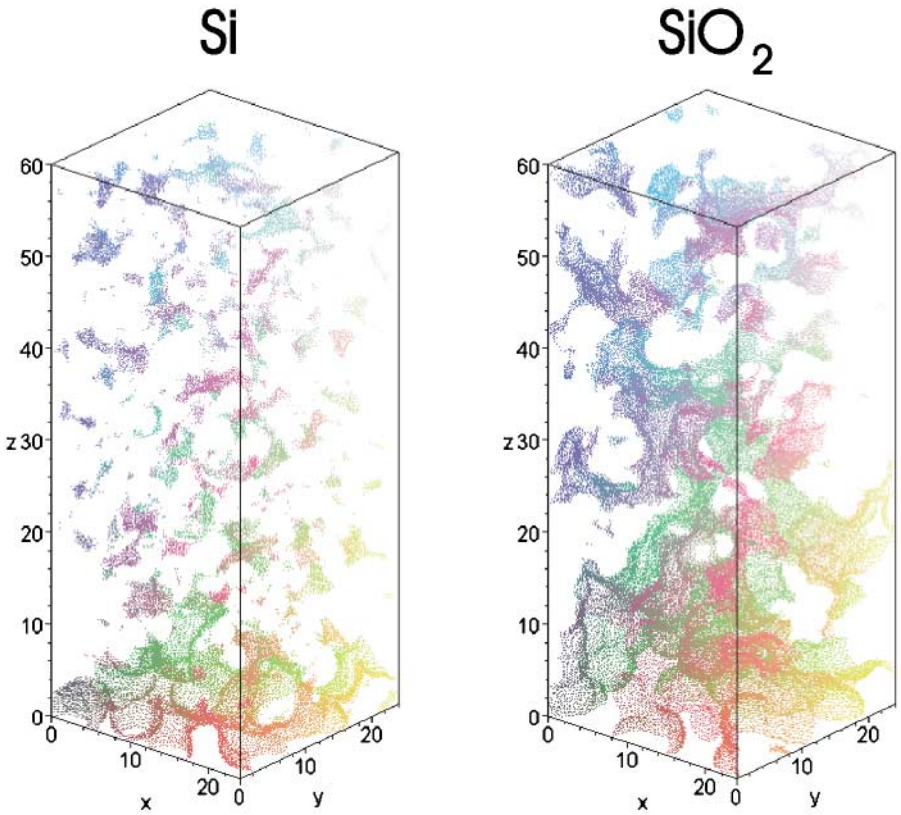

FIG. 3 (color). Simulated pore configurations in amorphous Si and SiO_2 films grown by vapor deposition. The surfaces of pores are revealed by colored points. Color is used solely to convey the three dimensionality of the porosity. In each case the substrate is at the bottom and periodic boundary conditions are applied along the x and y directions. The axes are in Å.

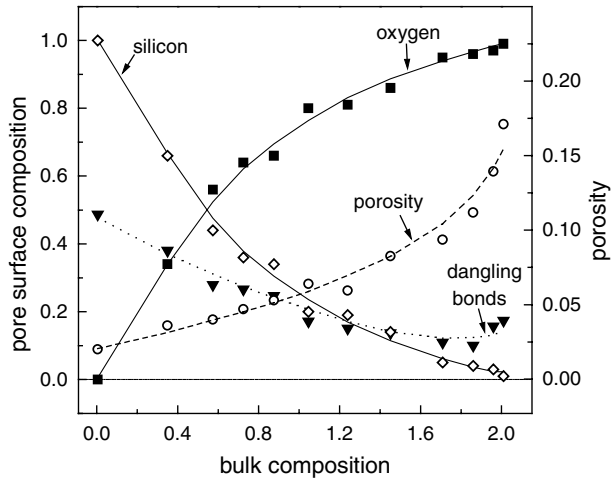

FIG. 4. The variations of the oxygen and silicon compositions of the pore surfaces, the fraction of all surface atoms with dangling bonds, and the fraction of the total volume of the film associated with pores, i.e., the porosity, with the oxygen composition x in SiO_x films, for a nucleation site density of 1.74 nm^{-2}.

$0 < x < 2$ on flat substrates as a function of the density of nucleation sites on the substrate. Our simulated radial distribution functions for SiO_2 and Si agree well with experimentally obtained distributions for bulk samples. As the oxygen content of the films increased the porosity increased, and the density of dangling bonds on the pore surfaces decreased, while the pore surfaces became covered with an increasing fraction of oxygen atoms. The oxygen appears to play the role of surfactant, lowering the energies of pore surfaces and enhancing the porosity of amorphous SiO_2 compared to pure amorphous Si. Since the ability of such films to prevent the permeation of gases depends on the porosity of the films, it is clearly of crucial importance that in any barrier film one takes into account the possibility of such surfactant behavior. We conclude that to reduce the porosity of these films one must either increase the density of nucleation sites on the substrate surface, or reduce the chemical potential of oxygen, for example by reducing its partial pressure in the vapor phase.

We thank Dr. I. Oleinik for useful discussions about dangling bond energies. This work was performed in the Oxford Toppan Centre, supported by the Toppan Printing Co., Ltd.

*On leave from the Institute for Spectroscopy, Russian Academy of Sciences, Troitsk, Moscow region, 142092, Russia.

[1] H. Chatham, Surf. Coat. Technol. **78**, 1–9 (1996).
[2] A. G. Erlat *et al.,* J. Phys. Chem. B **103**, 6047–6055 (1999).
[3] I. Tich, R. Car, and M. Parrinello, Phys. Rev. B **44**, 11 092–11 104 (1991).
[4] S. Susman *et al.,* Phys. Rev. B **43**, 1194–1197 (1991).
[5] J. F. Justo, M. Z. Bazant, E. Kaxiras, V. V. Bulatov, and S. Yip, Phys. Rev. B **58**, 2539–2549 (1998).
[6] F. Wooten, K. Winer, and D. Weaire, Phys. Rev. Lett. **54**, 1392–1395 (1985).
[7] Y. Tu, J. Tersoff, G. Grinstein, and D. Vanderbilt, Phys. Rev. Lett. **81**, 4899–4902 (1998).
[8] Y. Tu and J. Tersoff, Phys. Rev. Lett. **84**, 4393–4396 (2000).
[9] N. F. Mott and E. A. Davis, *Electronic Processes in Non-Crystalline Materials* (Clarendon, Oxford, 1979), 2nd ed.
[10] P. N. Keating, Phys. Rev. **145**, 637 (1966).
[11] D. D. Wagman and V. A. Medvedev, *CODATA Key Values for Thermodynamics* (Hemisphere Publishing Corp., New York, 1989).
[12] T. Uchino, Y. Kitagawa, and T. Yoko, Phys. Rev. B **61**, 234–240 (2000).
[13] S. Kugler *et al.,* Phys. Rev. B **40**, 8030–8032 (1989).
[14] R. de Daubeny, C. W. Bunn, and C. J. Brown, Proc. R. Soc. London A **226**, 531 (1954).
[15] A. Nakano, R. K. Kalia, and P. Vashishta, Phys. Rev. Lett. **73**, 2336–2339 (1994).
[16] J. V. L. Beckers and S. W. De Leeuw, J. Non-Cryst. Solids **261**, 87–100 (2000).